Supporting Information

The Influence of Linkers on Quantum Interference: A Linker Theorem

Yuta Tsuji,[1*] Thijs Stuyver,[2,3] Suman Gunasekaran,[4] Latha Venkataraman[4]

[1)] Education Center for Global Leaders in Molecular Systems for Devices, Kyushu University, Nishi-ku, Fukuoka 819-0395, Japan
[2)] Algemene Chemie, Vrije Universiteit Brussel, Pleinlaan 2, 1050 Brussels, Belgium (Member of the QCMM Ghent−Brussels Alliance Group)
[3)] Research Foundation-Flanders (FWO-Vlaanderen), Egmontstraat 5, 1000 Brussels, Belgium
[4)] Department of Applied Physics and Applied Mathematics and Department of Chemistry, Columbia University, New York, New York 10027, United States

*To whom correspondence should be addressed.
E-mail: yuta@ms.ifoc.kyushu-u.ac.jp

Table of contents

1. Dependence of the Green's function for the molecular part on the number of repeating units

To check whether the Green's function for the molecular part depends on the number of repeating units *n*, as an example, consider a polymer of 3 units. Its Hückel matrix can be written as

$$\mathbf{M}^{**} = \begin{pmatrix} \mathbf{m}^{*} & s & 0 \\ s & \mathbf{m} & s \\ 0 & s & \mathbf{m}^{*} \end{pmatrix}, \tag{S1}$$

where **m** represents the block matrix for the monomer unit. We assume that the monomers are linked together with a single bond, whose resonance integral is represented by *s*. This should hold true for most polymers. The upper left and lower right corners of the Hückel matrix include the self-energy terms due to the interaction with the electrodes/linkers, indicated by asterisk (*).

In accordance with eq. 25, one can obtain an expression for the Green's function for the molecular part by using Cramer's rule as follows:

$$G_{1,N}^{\mathbf{M}^{**}} = [E\mathbf{I} - \mathbf{M}^{**}]^{-1} = \frac{(-1)^{1+N}}{\det(E\mathbf{I}-\mathbf{M}^{**})}\Delta_{N,1}(E), \tag{S2}$$

where *N* indicates the number of atoms included in the molecular part and is an even integer for even alternant hydrocarbons. To calculate $\det(E\mathbf{I} - \mathbf{M}^{**})$, we can apply the matrix decomposition technique that we have done, by using eq. 4, in the main text to eliminate the linker parts. To obtain $\Delta_{N,1}(E)$, we use another matrix decomposition technique represented by eq. 2.

If one sequentially applies the matrix decomposition techniques to collapse the left

side of the secular determinant for the Hückel matrix, the element of the Green's function can then be reduced to

$$G_{1,N}^{\mathbf{M}^{**}} = g_{l,r}^{*(1)} \left(s \cdot {g_{l,r}}^{*^{(2)}}\right) \ldots \left(s \cdot {g_{l,r}}^{*^{(n-1)}}\right) \left(s \cdot {g_{l,r}}^{**}\right). \quad \text{(S3)}$$

This is exactly the same as what is done in eq. 30, but here we are only collapsing from the left. Each time we collapse the determinant, the Green's function of the monomer, which is represented by $g^{*^{(i)}}$, gets a self-energy term in the upper left corner of its matrix. These self-energy terms vary as the collapsing process goes on. Thus, the asterisks get a superscript ($*^{(i)}$) to differentiate each monomer Green's function from other ones. The self-energy term of the Green's function for the first monomer, $g^{*^{(1)}}$, comes from the linker/leads. Once one arrives at the final monomer, one finds that the Green's function includes two self-energy terms: one comes from the upper left matrix and the other one comes from the lower right matrix, i.e., right linker unit.

When the Hückel matrix for the monomer unit including the self-energy term due to the interaction with the left-neighboring monomer is denoted by $\mathbf{m}^{*^{(i)}}$, the Green's function for the monomer unit can be written as

$$g_{1,n}^{*(i)} = \left[E\mathbf{I} - \mathbf{m}^{*^{(i)}}\right]^{-1} = \frac{(-1)^{1+n}}{\det\left(E\mathbf{I} - \mathbf{m}^{*^{(i)}}\right)} \Delta_{n,1}(E), \quad \text{(S4)}$$

where *n* indicates the number of atoms in the monomer unit. Since the self-energy term is only included in the (1, 1) element of $\mathbf{m}^{*^{(i)}}$, $\Delta_{n,1}(E)$ is common among all monomers. For the case of the rightmost monomer, the self-energy term is included in both (1, 1) and (*n*, *n*) elements,

but this does not affect the value of $\Delta_{n,1}(E)$. As for $\det\left(E\mathbf{I}-\mathbf{m}^{*(i)}\right)$, one can use the cofactor expansion along the first column as follows:

$$\det\left(E\mathbf{I}-\mathbf{m}^{*(i)}\right)=\left(E-m_{1,1}-\sigma^{(i)}\right)\Delta_{1,1}+\sum_{i=2}^{n}\left(-m_{i,1}\right)(-1)^{i+1}\Delta_{i,1}, \quad \text{(S5)}$$

where $\sigma^{(i)}$ indicates the self-energy term. If the monomer unit is an even-alternant hydrocarbon, $\Delta_{1,1}(E)$ is equal to 0 when E = 0 because $\Delta_{1,1}(E)$ is an odd function.[1] This may not be true for the last monomer because it includes the self-energy term in the (n, n) element. However, if the coupling of the last monomer to the electrode/linker is not so large, the self-energy in the bottom right corner can be negligible. Thus, $\det\left(-\mathbf{m}^{*(i)}\right)$ is expected to be common among all monomers, and hence all of the monomer Green's functions are expected to be equal to the Green's function without the self-energy term, namely $g^{*(i)}=g$, when E = 0. This simplifies eq. S3 as follows:

$$G_{1,N}^{\mathbf{M}^{**}}=g_{l,r}^{*(1)}\left(s\cdot g_{l,r}^{*(2)}\right)\ldots\left(s\cdot g_{l,r}^{*(n-1)}\right)\left(s\cdot g_{l,r}^{**}\right)\approx\frac{1}{s}\left(s\cdot g_{l,r}\right)^{n}. \quad \text{(S6)}$$

Let us look at an example, polyene. The monomer unit is ethene and the Green's function at E = 0 can be written as

$$g_{1,2}=\left(-\begin{bmatrix}0 & d\\ d & 0\end{bmatrix}^{-1}\right)_{1,2}=\left(\begin{bmatrix}0 & -\frac{1}{d}\\ -\frac{1}{d} & 0\end{bmatrix}\right)_{1,2}=-\frac{1}{d}, \quad \text{(S7)}$$

where d indicates the resonance integral for the double bond in the monomer. By using eq. S4, one can obtain

$$\left|G_{1,N}^{\mathbf{M}^{**}}\right|^{2}=\left(\frac{1}{s}\left(s\cdot g_{l,r}\right)^{n}\right)^{2}=\frac{1}{s^{2}}\left(\frac{s}{d}\right)^{2n}. \quad \text{(S8)}$$

This equation agrees with the one in a previous study.[2] Plugging eq. S6 into the equation for

the exponential falloff, i.e., eq. 36, we can get

$$\beta_n = -\frac{\partial}{\partial n}\ln\left(\left|G_{1,N}^{\mathbf{M}^{**}}\right|^2\right) = -\frac{\partial}{\partial n}\ln\left(\left|\frac{1}{s}\left(s\cdot g_{l,r}\right)^n\right|^2\right) = -\ln\left(\left|g_{l,r}\cdot s\right|^2\right). \quad \text{(S9)}$$

This is a general formula for the decay constant of a polymer. This implies that the decay constant is equal to the transmission through the monomer multiplied by the coupling or resonance integral. Further, the exponential decay comes from the fact that the transmission through the polymer is the product of the transmission through the monomers. We can apply the formula of the exponential falloff to the polyene example, getting the same equation as the one derived in the previous study as follows:[2]

$$\beta_n = -\ln\left(\left|g_{l,r}\cdot s\right|^2\right) = -\ln\left(\left(-\frac{1}{d}\cdot s\right)^2\right) = -2\ln\left(\frac{s}{d}\right). \quad \text{(S10)}$$

As an aside, there is a slightly easier way to get the same formula. All one has to do is to realize that the decay constant is equal to the negative natural logarithm of the ratio between transmissions, T_n and $T_{n\text{-}1}$,

$$-\ln\left(\frac{T_n}{T_{n-1}}\right) = -\ln\left(\frac{e^{-\beta n}}{e^{-\beta(n-1)}}\right) = \beta_n. \quad \text{(S11)}$$

Therefore, to obtain the decay constant, one only needs to collapse one monomer unit as follows:

$$\frac{T_n}{T_{n-1}} \propto \frac{|G_n|^2}{|G_{n-1}|^2} = \frac{\left|(g_{l,r}\cdot s)G_{n-1}\right|^2}{|G_{n-1}|^2} = \left|g_{l,r}\cdot s\right|^2. \quad \text{(S12)}$$

Hsu and Rabitz[3] have derived another general relationship between the number of repeating units and the conductance decay constant. By following their scheme, we obtain an expression for the decay constant for conductance through polyenes as follows:

$$\beta_n = 2\ln\left|\frac{1}{\lambda_n}\right|, \tag{S13}$$

where λ_n is chosen so that its absolute value is the largest among the eigenvalues of the product of the monomer Green's function (**g**) and the coupling matrix between monomers (**v**). For the case of polyenes, the following equations hold true:

$$\mathbf{g} = \left(E\mathbf{I} - \begin{bmatrix} 0 & d \\ d & 0 \end{bmatrix}\right)^{-1}, \tag{S14}$$

and

$$\mathbf{v} = \begin{bmatrix} 0 & 0 \\ s & 0 \end{bmatrix}. \tag{S15}$$

This turns out to be the same as the formula we have derived above if one assumes that the monomers are linked by a single bond. Let us take a closer look at the explicit formula for the polyene example. The matrix **gv** can be written as

$$\mathbf{gv} = \left(E\mathbf{I} - \begin{bmatrix} 0 & d \\ d & 0 \end{bmatrix}\right)^{-1}\begin{bmatrix} 0 & 0 \\ s & 0 \end{bmatrix} = \begin{bmatrix} \frac{sd}{E^2-d^2} & 0 \\ \frac{Es}{E^2-d^2} & 0 \end{bmatrix}. \tag{S16}$$

The eigenvalues for this matrix are $\frac{sd}{E^2-d^2}$ and 0, so $\lambda_n = \frac{sd}{E^2-d^2}$, leading to

$$\beta_n = -2\ln\left(\frac{s}{d}\right), \tag{S17}$$

where we suppose that $E = 0$. As one can see in this example, if **v** only has an element in the bottom left corner, namely the assumption of the single-bond coupling, then the matrix **gv** only has nonzero elements in the first column. Therefore, the only nonzero eigenvalue is the 1st element of the matrix, $[\mathbf{gv}]_{1,1}$. Since the element $[\mathbf{gv}]_{1,1}$ is simply $g_{l,r} \cdot s$, the eigenvalues for **gv** are $g_{l,r} \cdot s$ and 0. Thus, we arrive at the same formula as derived above,

$$\beta_n = 2\ln\left|\frac{1}{\lambda_n}\right| = -\ln|\lambda_n|^2 = -\ln\left|g_{l,r} \cdot s\right|^2. \tag{S18}$$

So we can conclude that our methodology, which is based on the determinant decomposition technique, can provide a consistent result with the procedure developed by Hsu and Rabitz.

2. Extended Hückel calculations for the Fermi level alignment

We perform an extended Hückel calculation[4] to check how much the Fermi level in the substituted systems is different relative to the unsubstituted case. To this end, we hold up a diamino benzene molecule as an example. We carried out the geometry optimization of the *p*- and *m*-diamino benzene molecules with a single Au atom attached to each amine linker. The optimizations were performed at the B3LYP/LANL2DZ[5] level of theory by using the Gaussian 09 program.[6] The optimized *p*- and *m*-diamino benzene molecules with two Au atoms are bridged between two Au_{19} clusters which model an Au electrode. The structure of the constructed molecular junctions are shown in Figure S1. We performed transmission calculations for these molecular junctions at the extended Hückel level of theory by using YAeHMOP[7] and Artaios.[8]

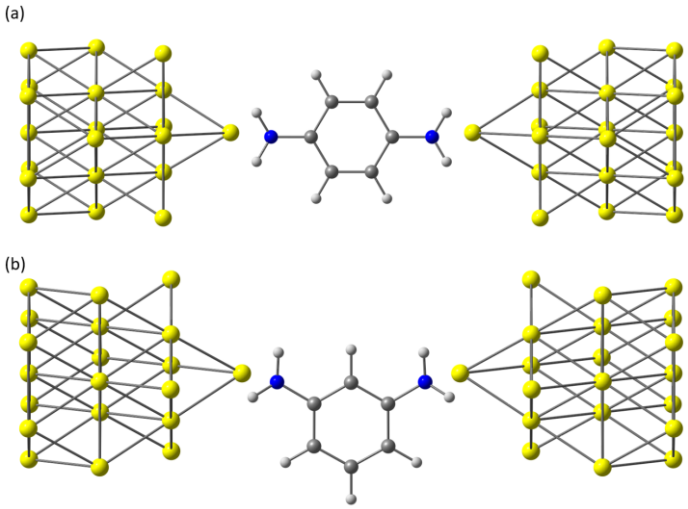

Figure S1. Structures of Au_{20}-*p*-diamino benzene-Au_{20} molecular junction (a) and Au_{20}-*m*-diamino benzene-Au_{20} molecular junction (b).

The calculated transmission spectra for the molecular junctions shown in Figure S1 are shown in Figure S2. One can clearly see a transmission dip at E = -11.1 eV in the transmission spectrum for *m*-diamino benzene, while one cannot see such a feature in that for *p*-diamino benzene. So the dip at E = -11.1 eV is considered to be due to quantum interference (QI).

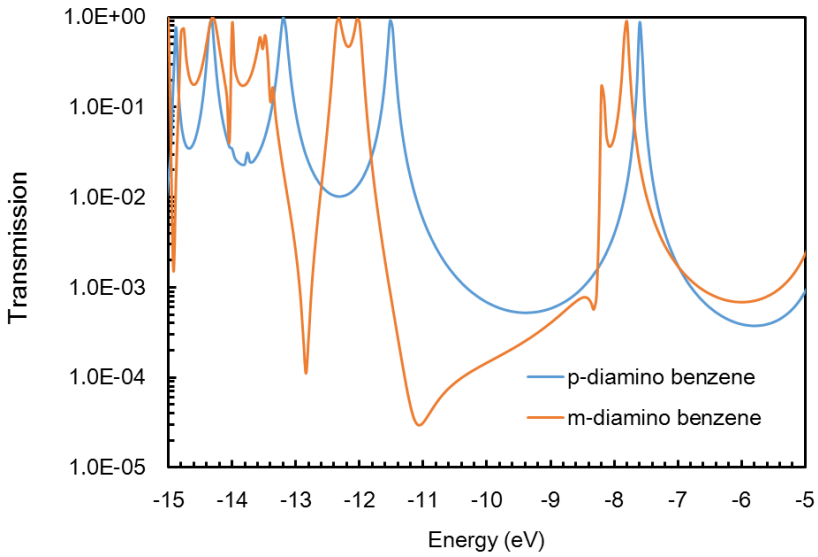

Figure S2. Transmission spectra calculated for Au_{20}-*p*-/*m*-diamino benzene-Au_{20} junctions at the extended Hückel level of theory.

In the extended Hückel theory, the energy level of carbon's $2p_z$ orbital, which is the extended-Hückel counterpart of carbons's Coulomb integral in the simple Hückel theory, is located at E = -11.4 eV. This energy level can be regarded as the Fermi level for molecular junctions consisting of an unsubstituted alternant hydrocarbon and is almost the same as the energy location of the QI dip. Therefore, the influence of overlap matrix and non-nearest

neighbor coupling, which is included in the extended Hückel method, does not affect the QI feature significantly.

In Figure S2 one can see a difference in transmission between molecular junctions with and without QI. In the energy region from -11.8 eV to -8.2 eV, the QI system has lower transmission than the non-QI system. This means that the transmission dip is not so narrow but as large as 3.6 eV. This is because the transmission dip appears in between the HOMO and LUMO of the bridged molecule, so the width of the dip can be comparable with the HOMO-LUMO gap. The HOMO-LUMO gap of the *p*- and *m*-diamino benzene molecules is in the range between 3.2 eV and 3.8 eV at the extended Hückel level of theory. As long as the HOMO-LUMO gap of the bridged molecule is larger than the estimated shift of the Fermi level, an experiment can at least detect the signature of QI.

To estimate the Fermi level of the gold electrodes, we carried out extended Hückel calculations for gold nano-clusters consisting of an odd-number of gold atoms. The structures of the smaller sized gold nano-clusters are taken from the ARTAIOS program, while those of the larger sized nano-clusters are generated by using Virtual NanoLab.[9] The structures of the generated clusters are shown in Figure S3.

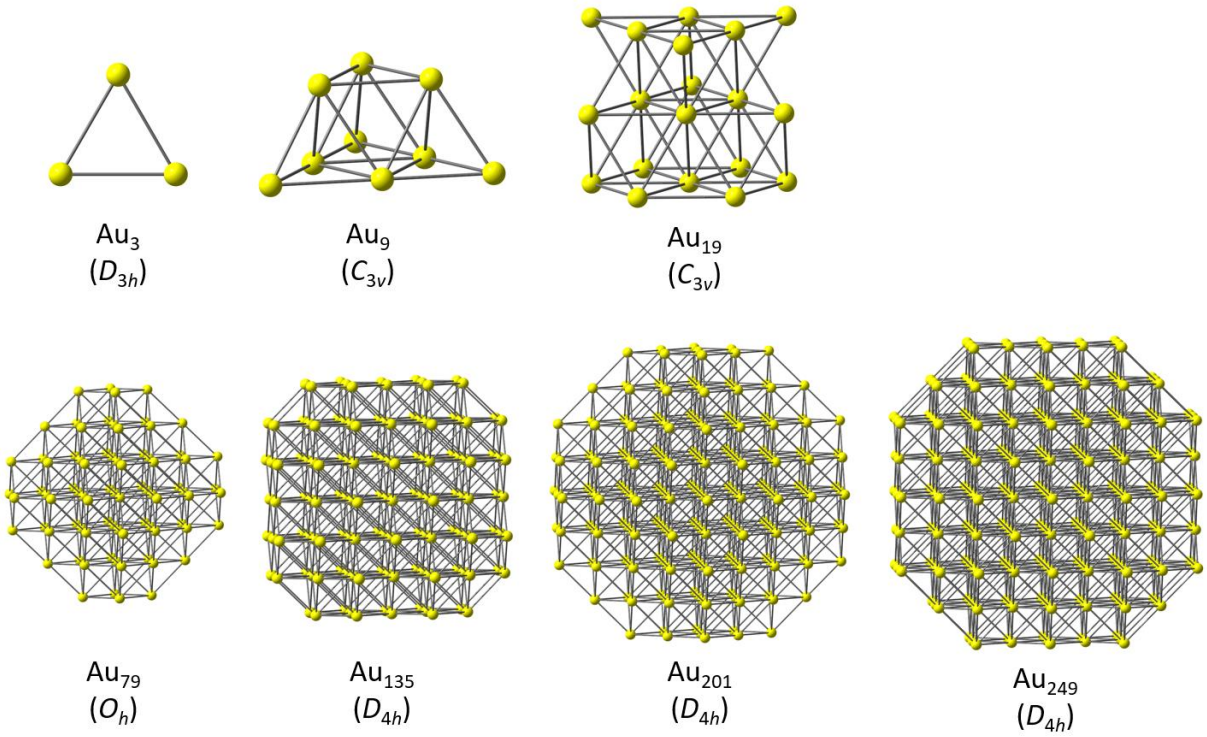

Figure S3. Structures of the smaller Au nano-clusters (top) and larger Au nano-clusters (bottom).

Since a gold atom includes odd-numbered valence electrons, odd-numbered gold clusters hold the singly occupied molecular orbital (SOMO), and it is reasonable to regard the SOMO level as the Fermi level of the gold cluster. Figure S4 shows a plot of the SOMO level as a function of the number of gold atoms included in the cluster. As the size of the cluster gets larger, the SOMO level converges to E = -10 eV. So we can conclude that the Fermi level of the gold electrode is located at around E = -10 eV. Thus, we find that the Fermi level in the substituted systems is different relative to the unsubstituted case by 1.4 eV in the case of the diamino benzene.

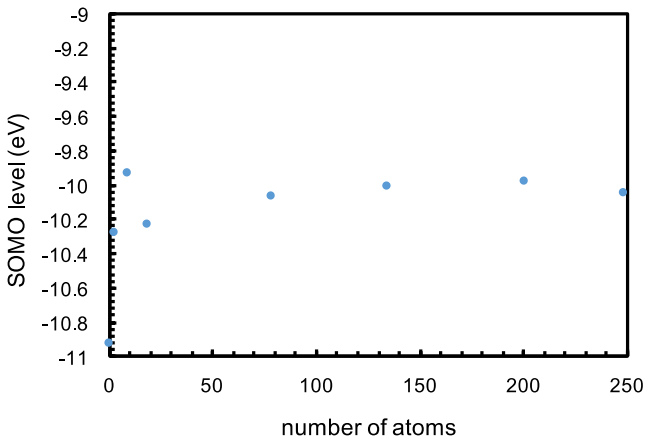

Figure S4. SOMO levels of Au nano-clusters calculated at the extended Hückel level of theory are plotted as a function of the number of Au atoms included in the cluster.

3. Supplementary references

(1) Stuyver, T.; Fias, S.; De Proft, F.; Geerlings, P. Back of the Envelope Selection Rule for Molecular Transmission: A Curly Arrow Approach. *J. Phys. Chem. C* **2015**, *119*, 26390-26400.

(2) Tsuji, Y.; Movassagh, R.; Datta, S.; Hoffmann, R. Exponential Attenuation of Through-Bond Transmission in a Polyene: Theory and Potential Realizations. *ACS Nano* **2015**, *9*, 11109-11120.

(3) Hsu, L.-Y.; Rabitz, H. Theory of Molecular Conductance Using a Modular Approach. *J. Chem. Phys.* **2016**, *145*, 234702.

(4) Hoffmann, R. An Extended Hückel Theory. I. Hydrocarbons. *J. Chem. Phys.* **1963**, *39*, 1397-1412.

(5) (a) Becke, A. Density-Functional Thermochemistry. III. The Role of Exact Exchange. *J. Chem. Phys.* **1993**, *98*, 5648-5652. (b) Lee, C.; Yang, W.; Parr, R. G. Development of the Colle-Salvetti Correlation-Energy Formula into a Functional of the Electron Density. *Phys. Rev. B* **1988**, *37*, 785-789. (c) Vosko, S.; Wilk, L.; Nusair, M. Accurate Spin-Dependent Electron Liquid Correlation Energies for Local Spin Density Calculations: A Critical Analysis. *Can. J. Phys.* **1980**, *58*, 1200-1211. (d) Hay, P. J.; Wadt, W. R. Ab Initio Effective Core Potentials for Molecular Calculations. Potentials for the Transition Metal Atoms Sc to Hg. *J. Chem. Phys.* **1985**, *82*, 270-283.

(6) Gaussian 09, Revision E.01, Frisch, M. J.; Trucks, G. W.; Schlegel, H. B.; Scuseria, G. E.; Robb, M. A.; Cheeseman, J. R.; Scalmani, G.; Barone, V.; Mennucci, B.; Petersson, G. A.; Nakatsuji, H.; Caricato, M.; Li, X.; Hratchian, H. P.; Izmaylov, A. F.; Bloino, J.; Zheng, G.; Sonnenberg, J. L.; Hada, M.; Ehara, M.; Toyota, K.; Fukuda, R.; Hasegawa, J.; Ishida, M.; Nakajima, T.; Honda, Y.; Kitao, O.; Nakai, H.; Vreven, T.; Montgomery, Jr., J. A.; Peralta, J. E.; Ogliaro, F.; Bearpark, M.; Heyd, J. J.; Brothers, E.; Kudin, K. N.; Staroverov, V. N.; Kobayashi, R.; Normand, J.; Raghavachari, K.; Rendell, A.; Burant, J. C.; Iyengar, S. S.; Tomasi, J.; Cossi, M.; Rega, N.; Millam, J. M.; Klene, M.; Knox, J. E.; Cross, J. B.; Bakken, V.; Adamo, C.; Jaramillo, J.; Gomperts, R.; Stratmann, R. E.; Yazyev, O.; Austin, A. J.; Cammi, R.; Pomelli, C.; Ochterski, J. W.; Martin, R. L.; Morokuma, K.; Zakrzewski, V. G.; Voth, G. A.; Salvador, P.; Dannenberg, J. J.; Dapprich, S.; Daniels, A. D.; Farkas, Ö.; Foresman, J. B.; Ortiz, J. V.; Cioslowski, J.; Fox, D. J. Gaussian, Inc., Wallingford CT, 2009.

(7) Landrum, G. A.; Glassey, W. V. YAeHMOP: Yet Another extended Hückel Molecular Orbital Program. YAeHMOP is available free of charge via the WWW at URL: https://sourceforge.net/projects/yaehmop/

(8) Herrmann, C.; Groß, L.; Steenbock, T.; Solomon, G. C. *Artaios version 0.3.0*, 2014.

(9) Virtual NanoLab version 2015.1, QuantumWise A/S (www.quantumwise.com)